SPH Free Surface Flow Simulation

M. Doring,Y. Andrillon, B. Alessandrini, P. Ferrant
Laboratoire de Mécanique des Fluides, UMR-CNRS 6598
Ecole Centrale de Nantes
mathieu.doring@ec-nantes.fr

Abstract

This paper presents the use of a SPH method in different free surface flow simulations. Results are compared with experimental data when available, and with results obtained using a "Volume Of Fluid" approach. Simulations shows a good agreement with experiments and confirms the ability of SPH method to simulate complex free surface flows. However improved boundary conditions are still needed.

Introduction

Free surface flow simulation sees its limits unceasingly pushed further. One of the last great difficulty in this domain has been the problem of reconnection of interfaces, occurring in flows with breaking waves. Within the last ten years, with the advent of the free surface capturing methods initiated by Hirt & Nichols[4] the numerical solution of these flows has become possible. Nevertheless, another approach has been recently introduced to simulate this kind of flow. This approach, named "Smooth Particles Hydrodynamics", was first applied to free surface flows by Monaghan[8]. Being meshless and Lagrangian, SPH is well adapted in the simulation of complex flows. In this paper we present some results obtained using a SPH method compared both with experimental data and with results obtained using a "Volume Of Fluid" approach.

SPH Solver

In SPH type methods a set of interpolating points is chosen in the medium. These points are associated with an interaction function (Kernel function) which is used to discretise the partial differential operators. In the case of free surface flows, the equations to be solved are Navier-Stokes equations (1, 2) and an equation of state for the pressure called Tait's equation (3). SPH is usually a compressible Lagrangian method, but if the Mach number remains below 0.1 during the whole simulation, the flow can be regarded as incompressible.

$$\frac{d\vec{v}}{dt} = \vec{g} - \frac{\nabla P}{\rho} + \overrightarrow{a_{viscous}} \quad (1)$$

$$\frac{d\rho}{dt} = -\rho.\nabla.\vec{v} \quad (2)$$

$$P = \kappa((\frac{\rho}{\rho_0})^7 - 1) \quad (3)$$

$$W(q = \frac{|\vec{r}|}{h}) = C \begin{cases} \frac{2}{3} - q^2 + \frac{1}{2}q^3 & \text{if } 0 \leq q < 1 \\ \frac{1}{6}(2-q)^3 & \text{if } 1 \leq q < 2 \\ 0 & \text{else} \end{cases} \quad (4)$$

To discretise the previous equations, variables are convoluted with the kernel function which tends to a Dirac distribution. In this paper the chosen kernel is the cubic spline kernel introduced by Monaghan (4), where C is a constant set to ensure $\int W = 1$. Then the values of a function and its gradient can be determined in the following way :

$$f(\vec{r}) \approx \int_D f(\vec{x}) W(\vec{r} - \vec{x}) d\vec{x} \qquad \nabla f(\vec{r}) \approx \int_D \nabla f(\vec{x}) W(\vec{r} - \vec{x}) d\vec{x} = \int_D f(\vec{x}) \nabla W(\vec{r} - \vec{x}) d\vec{x} \quad (5)$$

The second equation is obtained via integration by parts by neglecting the surface term which is null for interior particles as kernel function cancels itself for $\frac{|\vec{r}|}{h} \geq 2$.

This kind of discretisation is second order in space, and to enhance the numerical performance, such as conservation of linear momentum, the formulae are symmetrized [7] leading to the following scheme, where i-subscripted variables correspond to the i^{th} particle :

$$\frac{d\vec{x_i}}{dt} = \vec{v_i} \quad (6)$$

$$\frac{d\vec{v_i}}{dt} = \vec{g} - \Sigma_j \, m \, (\frac{P_i}{\rho_i^2} + \frac{P_j}{\rho_j^2}) \nabla W(\vec{r_i} - \vec{r_j}) \quad (7)$$

$$\frac{d\rho_i}{dt} = -\Sigma_j \, m \, (\vec{v_i} - \vec{v_j}) \, \nabla W(\vec{r_i} - \vec{r_j}) \quad (8)$$

This ordinary differential equation system can be integrated in time by schemes such as Runge-Kutta, Leap-Frog, Predictor-Corrector to ensure second order convergence in time.

Results

In order to evaluate the performances of SPH methods in the simulation of free surface flows, a few test cases were simulated and results compared with experimental data when available and with results obtained by a VOF method using the Fully Coupled technique [1] [2] . These test cases are sloshing tank, dam breaking, and dam breaking with obstacle.

Sloshing tank

The first test case can be defined as follows : a rectangular tank of 0,4 m wide and 0,2 m high, filled with 60 percent of water (0.12 m high) , is forced to oscillate from left to right. The water begins to move in an oscillatory way before impacting the top wall. Experimental free surface shapes are available before the first impact on top wall[3]. The tank is moved in an horizontal plane as follows :

$X(t) = A_0\,[sin(2\,\pi\,f_1\,t) - sin(2\,\pi\,f_2\,t]$ with $A_0 = 0.0075m$, $f_1 = 1.598Hz$ and $f_2 = 1.307Hz$

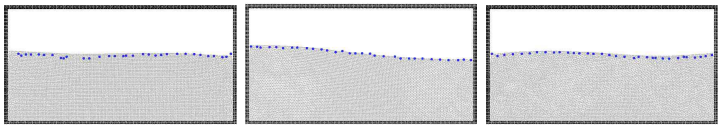

(a) t=0,45 s , t=0,6 s et t=0,75 s

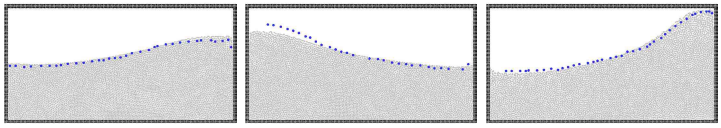

(b) t=0,96 s , t=1,23 s et t=1,65 s

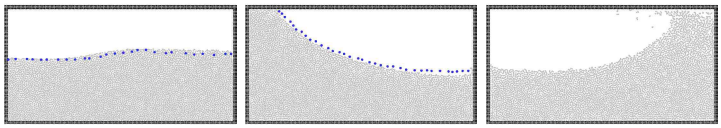

(c) t=1,83 s , t=2 s et t=2.34 s

FIG. 1: Comparison between numerical (grey) and experimental (black) free surface shape

As can be seen in previous figures,computed free surface shapes are in good agreement with those extracted from experiments(black dots). However, the figure 3 shows that for low resolution (81x25 particles), the SPH solver predicts an impact on the upper boundary at time $t = 1.652$ s. This can be explained by the fact that the experimental free surface is very close to the upper boundary at this time (about 5 mm), and the interaction distance for particles is greater (approximately 12 mm and 6mm for respectively 81x25 and 163x49 particles) leading to the impact ; but it seems that this impact has negligible influence on later times for the 163x49 simulation.

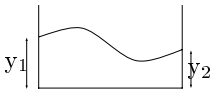

FIG. 2: y_1 and y_2 definition

Dam breaking

Dam breaking is typically employed to demonstrate the ability of codes to compute transient fluid flow with breaking free surface. The corresponding experiment has been made by Martin and Moyce[5], and more recently by Koshizuka[6]. The initial water column is 0.146 m wide and 0.292 m high, and the tank is 0.584 m wide. The flow, at first stage, presents the collapse of the column with a tongue of fluid propagating towards the opposite wall of the tank. Then the fluid strikes the right vertical wall, and goes up along it. During the next stage a breaking wave moves backward, then the flow is damped as in a sloshing tank. Data available from the experiment consists in pictures which show the time evolution of the breaking water wave, and secondary data such as the position of the wave front on the vertical and horizontal walls. The comparisons between numerics and experiments are presented in figures 5 and 6,where a is the water column initial width. If the simulated position on the left vertical wall is in good agreement with the experimental one, the position of the wave front on the

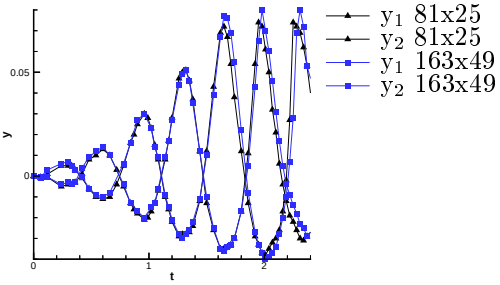

FIG. 3: temporal evolution of y_1 and y_2

horizontal wall is less accurate. The "VOF" and the "SPH" show the same advance on the experimental result. This difference could probably be explained by the wall slip condition used in cor

This difference does not appear on the vertical wall, due to a lower speed. Another explanation is linked to the capturing of the interface. On the horizontal wall the tongue of water is so thin that the calculation in the VOF method of the iso-value $c = 0.5$ position is dubious. And, for the same reason it is difficult to find precisely the interface in the distribution of particles in the "SPH" method. In figure 7 the temporal evolution of the leading edge on the right

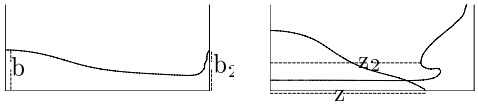

FIG. 4: secondary data description

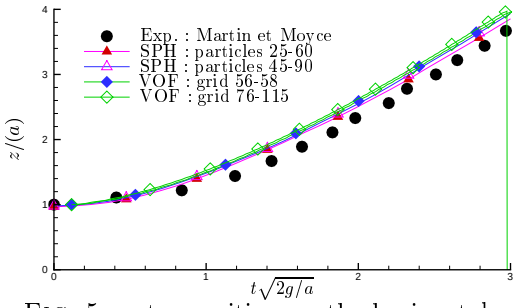

FIG. 5: water position on the horizontal wall

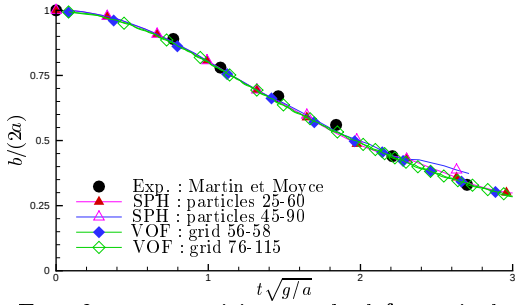

FIG. 6: water position on the left vertical wall

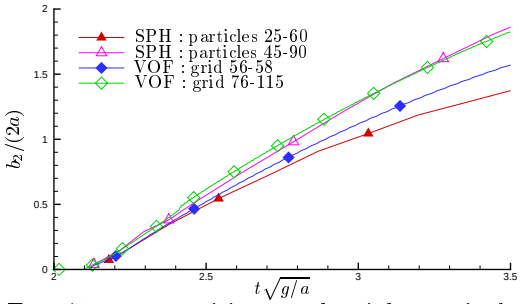

FIG. 7: water position on the right vertical wall

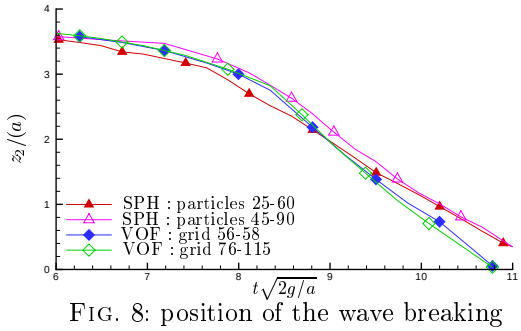

FIG. 8: position of the wave breaking

vertical wall is followed. Stronger differences appear between the different configurations of grid, and of numbers of particles respectively. These differences can be explained in the same manner as for the horizontal front wave evolution and are increased by the thinness of the water on the wall. The fourth characteristic of the flow studied is the speed of the backward wave. In this case the two set of numerical data are similar. Unfortunately, there is no experimental data to validate this result.

(a) Experiments

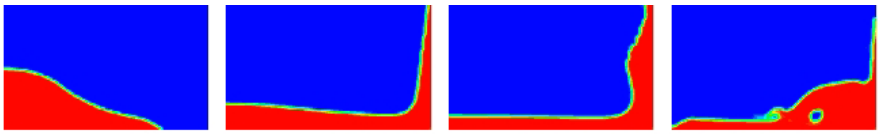

(b) VOF simulation

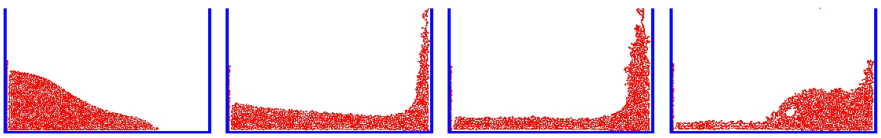

(c) SPH simulation

FIG. 9: free surface at $t = 0.2$ s,$t = 0.4$ s,$t = 0.6$ s and $t = 0.8$ s

As mentioned above, different pictures of the flow are available, and figures 9(a), 9(b) and 9(c) present respectively the experimental free surface profiles the two corresponding numerical results. Globally, the free surface profiles given by the numerical simulations are close to the experimental one, although the size of the entraped bubble is underestimated in the SPH calculation. But, one has to remember that the SPH code is a one single fluid solver and consequently the influence of the second fluid is neglected. However, it has been remarked that by increasing the number of particles the size of the bubble is more and more accurate. More simulations are thus necessary to explain the origin of this difference.

Dam breaking with obstacle

This third test case uses the same geometry defined before, with the addition of an obstacle. This results in a more complex flow. In practice, after the leading edge reaches the obstacle a tongue of fluid continues its motion towards the opposite wall, and the impact of the fluid on the wall is more violent. In this application, during the first 0.4 s the flow of the different numerical simulations is in good agreement with the experimental data. After 0.5 s, the free surface evolution of the SPH is less accurate than the VOF one. Practically, the tongue of water connecting the obstacle and the right wall falls down abnormally. The explanation of this phenomena is the same as for the under estimating of the bubble in the previous application. Figure 10(c) gives the pressure field in both air and water. The difference of pressure between the two sides of the tongue of water hitting the right wall is clearly depicted, confirms that the influence of air on the water flows cannot be neglected, which explains the difference between VOF and SPH results.

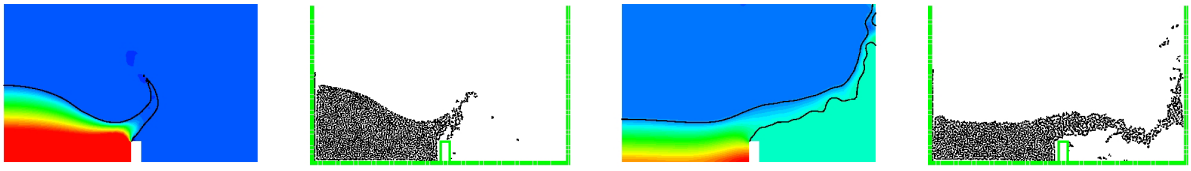

(a) VOF simulation (b) SPH simulation (c) VOF simulation (d) SPH simulation

FIG. 10: Free surface at $t = 0.2$ s and $t = 0.35$ s

Conclusion

Comparisons given in this paper demonstrate the ability of the SPH method to simulate complex free surface flows, and the accuracy of the SPH results against experimental and VOF simulation, including local flow characteristics such as the position of the leading edge on the wall. However, as in the SPH simulation the influence of the second fluid is neglected, some flow details are inaccurately predicted such as the flow with fluid 2 confined in a bubble. Then future work will be devoted to the inclusion of a second fluid in the SPH method, and the improvement of the numerical treatment of boundaries . 3D applications are also planed in the longer term.

Références

[1] Y. Andrillon and B. Alessandrini. A 2D+T VOF fully coupled formulation for calculation of breaking free surface flow. In *24th Symposium on Naval Hydrodynamics*. July 2002.

[2] Y. Andrillon and B. Alessandrini. A fully-coupled VOF method for free surface simulation. In *Proc 17th International Workshop on Water Waves and Floating Bodies*. R C T Rainey editor. April 2002.

[3] P. Corrignan. *Analyse Physique des Phénomènes Associés au Ballotement de Liquide dans des Réservoirs (Sloshing)*. Ph.D. thesis, Ecole Centrale de Nantes, Novembre 1994.

[4] C. W. Hirt and B. D. Nicholls. Volume of fluid (VOF) method for the dynamics of free boundaries. *Journal of Computational physics*, 39 :201–225, 1981.

[5] W. J. M. J C Martin and. An experimental study of the collapse of liquid columns on a rigid horizontal plane. *Philos. Trans. Soc. London*, A244 :312–324, 1952.

[6] S. Koshizuka and Y. Oka. Moving particle semi-implicit method : Fully lagrangian analysis of incompressible flows. In *European Congress on Computational Methods in Applied Sciences and Engineering*. ECCOMAS, 2000.

[7] J. J. Monaghan. Smoothed particle hydrodynamics. *Annu. Rev. Astron. Astrophys.*, 30 :543–574, 1992.

[8] J. J. Monaghan. Simulating free surface flows with sph. *Journal of Computational physics*, 110 :399–406, 1994.